Development and analysis of a new integrated power and cooling plant using LiBr–H_2O mixture

R SHANKAR and T SRINIVAS*

Energy Division, CO_2 Research and Green Technologies Centre, School of Mechanical and Building Sciences, VIT University, Vellore 632 014, India
e-mail: srinivastpalli@yahoo.co.in

MS received 16 September 2013; revised 21 March 2014; accepted 25 March 2014

Abstract. Cooling needs are increasing rapidly at hot climatic countries with increased global warming. The existed vapour compression refrigeration (VCR) system demands electricity for its operation which is more expensive. The concept of a newly proposed cooling cogeneration cycle has been developed by clubbing the power and cooling processes. It consists of characteristics of Rankine cycle and vapour absorption refrigeration (VAR) system and can be developed at hot climatic conditions with LiBr–water mixture as a working fluid. The results show that increase in heat source temperature is boosting power with a drop in cooling. The resulted cooling is seven times more than the power generation. The separator temperature has been recommended from 140 to 150°C to maximize the total output.

Keywords. Cooling; combined; integration; power; thermal.

1. Introduction

It is difficult to erect conventional power plants to meet the increased power and cooling loads due to its exhaustive in nature. Decentralized power system, waste heat recovery and cogeneration system, etc.; are the alternative roots to solve this problem. In cooling cogeneration (common plant for power and cooling) a considerable save in power consumption is due to generation of cooling without electrical input. It is not possible to operate a steam power plant at low temperature heat source but steam can be generated in a low temperature and low pressure operated LiBr–H_2O based vapour absorption refrigeration (VAR) system with a high coefficient of performance (COP) compared to aqua ammonia mixture. If these two configurations are clubbed together, it is possible to generate power at low temperature heat source which is not possible in a power station alone. In this work, an integrated plant has been designed and studied in thermodynamic point of view to check its feasibility at hot climatic conditions with LiBr–H_2O mixture. It is compact in size compared to couple plants (Sreeramulu *et al* 2011; Srinivas *et al* 2011, 2012; Srinivas & Vignesh 2012) due to sharing of some components.

*For correspondence

Ishida *et al* (1991) invented a new power cycle by modifying the LiBr–water based VAR plant. This is a typical vapour absorption power cycle similar to Kalina cycle system which generates the power at 300°C of source temperature. Goswami cycle is an integrated plant which generates power and cooling in which evaporator is located at exit of the turbine (Tamm *et al* 2003, 2004; Tamm & Goswami 2003). Vidala *et al* (2006) applied exergy method to evaluate the Goswami cycle by parametric variations. It is suitable for cold climatic conditions where the sink temperature is low to get enough cooling at the evaporator. It will not result much cooling with high sink temperature at hot climatic conditions. So there is a need to develop a novel and suitable integrated plant for places of hot climate. In the proposed design, refrigeration effect has been obtained from the vapourization of low temperature liquid refrigerant instead of low temperature vapour at the evaporator. Many researchers have developed, modelled, simulated, analysed, designed and experimented on LiBr–H_2O based cooling cycle where LiBr is an absorbent and water/steam is the refrigerant (Talbia & Agnew 2000; Misra *et al* 2003; Aphornratana & Sriveerakul 2007).

Novel technologies such as micro turbines, fuel cells, stirling engines, innovative absorption chillers, adsorption chillers and dehumidifiers are emerging in small scale distributed cogeneration units. Zheng *et al* (2006) developed a novel absorption power and cooling cycle and reported 24% of cycle efficiency at a maximum temperature of 350°C. But the cycle proposed is a complex in nature. Wang *et al* (2008) designed a combined power and refrigeration cycle which combines the Rankine cycle and the absorption refrigeration cycle. They reported a cycle efficiency of 20.5% at the source temperature of 300°C. Wang *et al* (2009) also proposed a new combined power and ejector absorption refrigeration cycle, which combines the Rankine cycle and the ejector absorption refrigeration cycle, and could produce both power output and refrigeration output simultaneously. They resulted in 21% of thermal efficiency at the source temperature of 300°C. Jawahar *et al* (2013) have shown the results of 225 kW of cooling and 80 kW power from aqua ammonia based integrated system. They attained a maximum combined thermal efficiency of 35–45% and coefficient of performance of about 0.35 at the optimum conditions. Zhang *et al* (2011) developed the concept of new trigeneration system that can recover the heat of the LiBr refrigeration cooling water from heat water boiler with high COP.

The literature survey shows that not much effort has been done towards the development of an integrated plant to suit for hot climatic conditions. Most of the integrated plant concepts are developed with aqua ammonia as a working fluid. LiBr–water has not yet been developed as working fluid for the integrated plant. It may be due to the operation of cooling system completely under vacuum. The proposed design overcomes this difficulty as the high pressure (HP) is maintained at 4 bar (at 200°C) instead of vacuum. It gains the benefits of high heat content of steam and high COP. The main objective of this work is to examine the thermodynamic feasibility and development of optimum operational conditions. The identified key parameters are strong solution concentration, separator's temperature and sink temperature. Kaita (2001), Sun (1997) and Florides *et al* (2003) developed thermodynamic properties for LiBr/H_2O mixture and these equations have been used to evaluate the proposed plant. The focused results are energy utilization factor (EUF) for cycle and plant, specific power, specific cooling, power cycle efficiency, cycle coefficient of performance (COP), total output and collector specific area.

2. Methodology

The proposed cooling cogeneration plant has been evaluated in view of the first and second law of thermodynamics. The mass, energy and exergy balances and its formulation have been

developed to solve the whole plant with suitable assumptions. The schematic flow diagram shows the processes details for the proposed plant with solar-assisted energy (figure 1). Thermodynamic processes and its properties can be studied from figure 2a (enthalpy–concentration diagram) and 2b (temperature–entropy diagram). These values at the state points are also tabulated in table 1.

The dryness fraction (vapour mass to total mass) values have been tabulated to know the condition of working fluid at each state of cycle. For a working fluid, dryness fraction 0 indicates a liquid, 1 indicates a vapour and the value between 0 and 1 gives the liquid–vapour mixture. The superheated vapour (1) expands through mixture turbine and generates power. Since it is expanded (2) to IP which is a function of sink temperature, it should be cooled from superheated vapour to saturated liquid condition in a condenser. The liquid will expand through throttling valve (4–5) and results a wet mixture with low dryness fraction after rejecting heat to vapour at subcooler. The low temperature fluid (5) is capable of absorbing heat in evaporator from surroundings. The dry steam (6) again absorbs heat at subcooler and mixed with strong solution (15) at the absorber inlet due to absorption action with strong solution. The mixed stream (8) again

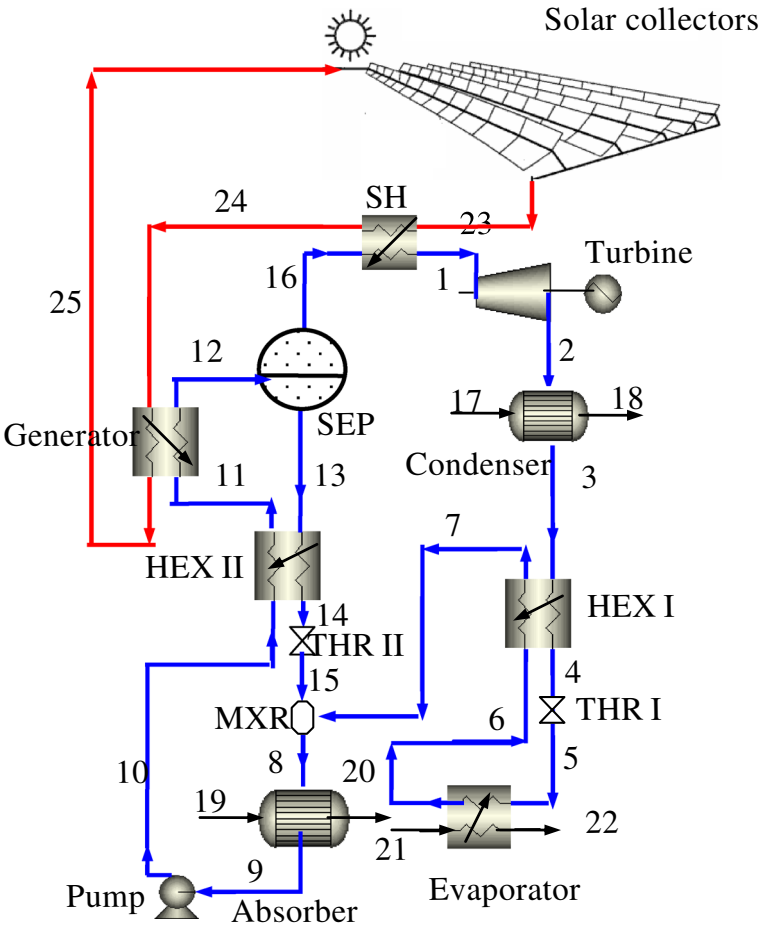

Figure 1. Schematic arrangement of cooling cogeneration plant.

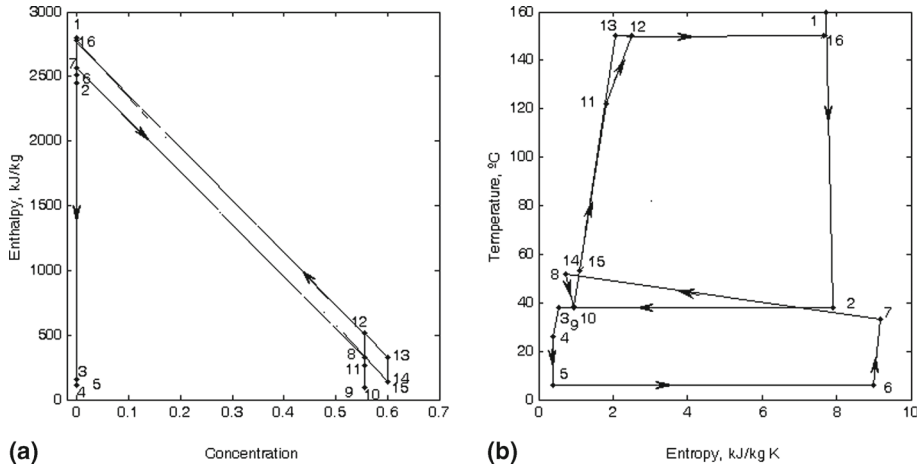

Figure 2. (**a**) Enthalpy–concentration and (**b**) temperature–entropy diagram for the cooling cogeneration cycle shown in figure 1.

Table 1. Solar thermal integrated plant material flow details with respect to figure 1 at $T_{sep} = 150°C$ and 60% of strong solution concentration.

State	Pressure (bar)	Temperature (°C)	LiBr concentration	Flow rate (kg s^{-1})	Specific enthalpy (kJ kg^{-1})	Specific entropy (kJ kg^{-1} K^{-1})	Specific exergy (kJ kg^{-1})	Dryness fraction
1	0.89	160.00	0.00	0.075	2796.92	7.72	496.68	1.00
2	0.07	39.94	0.00	0.075	2451.00	7.91	92.26	1.00
3	0.07	38.00	0.00	0.075	159.09	0.55	−3.50	0.00
4	0.07	26.04	0.00	0.075	109.10	0.38	−4.65	0.04
5	0.01	6.00	0.00	0.075	109.10	0.39	−7.72	1.00
6	0.01	6.00	0.00	0.075	2512.57	9.00	−171.21	1.00
7	0.01	33.00	0.00	0.075	2562.82	9.17	−172.19	1.00
8	0.01	51.50	0.55	1.000	324.09	0.73	107.93	1.00
9	0.01	38.00	0.55	1.000	91.19	0.95	−192.12	0.00
10	0.89	38.27	0.55	1.000	91.25	0.95	−192.95	0.00
11	0.89	122.09	0.55	1.000	264.00	1.81	−276.44	0.00
12	0.89	150.00	0.55	1.000	513.02	2.49	−228.83	0.07
13	0.89	150.00	0.60	0.925	328.15	2.07	−287.57	0.00
14	0.89	53.27	0.60	0.925	141.30	1.12	−192.02	0.00
15	0.01	53.01	0.60	0.925	141.30	1.12	−192.12	0.00
16	0.89	150.00	0.00	0.075	2777.16	7.67	490.68	1.00
17	–	30.00	–	1.343	20.90	0.07	0.17	–
18	–	38.00	–	1.343	54.34	0.18	1.15	–
19	–	30.00	–	1.808	20.90	0.07	0.17	–
20	–	38.00	–	1.808	54.34	0.18	1.15	–
21	–	11.00	–	4.539	−58.52	−0.20	1.42	–
22	–	6.00	–	4.539	−79.42	−0.28	2.64	–
23	–	185.00	–	1.581	560.00	1.80	133.40	–
24	–	175.00	–	1.581	525.00	1.70	119.11	–
25	–	147.09	–	1.581	427.32	1.43	82.58	–

condensed in the absorber to result a saturated liquid (9). The liquid solution is then pumped (9–10) to generator pressure (high pressure) via solution heat exchanger. The hot fluid coming from the solar concentrating collectors (23) is used to generate liquid vapour mixture (12) in generator and superheated vapour (1) at superheater. The strong solution (13) after rejecting heat at solution heat exchanger, throttled to LP mixture (15). It is mixed with vapour at exit of evaporator and repeats the cycle for continuous supply of power and cooling.

The following are the assumptions used in the evaluation of compound (power and cooling) plant. The reference thermodynamic state is taken as 25°C and 1.01325 bar. Solar radiation has been considered at 700 Wm^{-2} of beam and 950 Wm^{-2} of global radiation at the location (Vellore, India). The weak solution flow rate (m_8) is assumed as 1 kgs^{-1}. The separator temperature is 150°C. Terminal temperature difference (TTD) in superheater is 25 K. The TTDs for condenser and absorber are 10 and 8 K, respectively. Degree of superheat (DSH) in superheater is 10 K. Isentropic efficiency of steam turbine is 85%. The mechanical efficiency of turbine and pump is taken as 96%. Generator efficiency is 98%. The circulating cooling water inlet temperature for condenser and absorber is considered as 30°C. The evaporator (cooling chamber) exit temperature has been considered at 6°C. Pressure drop and heat losses in heat exchangers and pipelines are neglected.

The evaluation method has been detailed in the following section with formulation. The HP in the plant has been determined from the separator liquid temperature and its concentration assuming it as saturated liquid. The intermediate pressure (IP) is determined from the saturated water temperature at the condenser exit. The steam condition at the evaporator exit has been assumed as saturated vapour condition. From the saturated temperature of evaporator, the low pressure (LP) can be determined.

From the mass balance equations, it can be found that

$$\text{Circulation ratio, } \lambda = \frac{m_{ss}}{m_{ref}} = \frac{x_{ws}}{x_{ss} - x_{ws}} = \frac{m_{13}}{m_7} = \frac{x_{12}}{x_{13} - x_{12}}. \tag{1}$$

The weak solution concentration can be obtained at the absorber exit condition (temperature and pressure). The circulation ratio has been obtained from Eq. (1) at the assumed strong solution concentration. It gives the refrigerant mass (water/steam) at unit mass of weak solution.

At absorber

$$\mathrm{m_{ws}} = \mathrm{m_{ss}} + \mathrm{m_{ref}}, \tag{2}$$

$$\text{i.e., } m_8 = m_{13} + m_7, \tag{3}$$

Let $m_{\mathrm{ws}} = m_8 = 1\ \mathrm{kgs^{-1}}$, then

$$m_{ref} = \frac{m_{ws}}{1+\lambda}, \tag{4}$$

$$\text{i.e., } m_1 = \frac{m_8}{1+\lambda}, \tag{5}$$

$$m_{ss} = \lambda m_{ref} = \lambda \left(\frac{m_{ws}}{1+\lambda} \right), \tag{6}$$

$$\text{i.e., } m_{13} = \lambda \left(\frac{m_8}{1+\lambda} \right), \tag{7}$$

The vapour fraction,

$$VF = \frac{m_{16}}{m_{12}} = \frac{1}{1+\lambda}, \tag{8}$$

$$\mathrm{T_{17}} = \mathrm{T_1} + \mathrm{TTD_{SH}}. \tag{9}$$

The temperature of working fluid before throttling,

$$T_{14} = T_{10} + TTD_{\text{solution HEX}}. \tag{10}$$

From energy balance in solution heat exchanger,

$$h_{11} = h_{10} + \frac{m_{13}(h_{13} - h_{14})}{m_{11}}. \tag{11}$$

The temperature of steam at exit of subcooler,

$$T_7 = T_3 - TTD_{\text{subcooler}} \tag{12}$$

From energy balance in subcooler,

$$h_4 = h_3 - (h_7 - h_6). \tag{13}$$

T_4 can be iterated from the h_4.

At the mixing of streams before absorber,

$$h_8 = \frac{m_{15}h_{15} + m_7h_7}{m_8}. \tag{14}$$

The hot thermic fluid temperature at the generator exit,

$$T_{25} = T_{11} + TTD_{\text{HRVG}}. \tag{15}$$

The demand of hot fluid per unit mass of weak solution from the energy balance in the generator,

$$m_{23} = \frac{m_{11}(h_{12} - h_{11}) + m_1(h_1 - h_{16})}{c_{ph}(T_{23} - h_{25})}. \tag{16}$$

Design features of parabolic trough collector with vacuum tube at the focal line have been collected from the manufacturer's specifications. The collector length in row can be determined from the collector's efficiency and outlet temperature of the fluid.

Parabolic trough collector efficiency (Valan Arasu & Sornakumar 2007),

$$\eta_c = 0.642 - 0.441\left(\frac{T_{fi} - T_a}{R_b}\right). \tag{17}$$

Length of each parallel line,

$$L = \frac{m_{23}c_{ph}(T_{23} - T_{25})}{\eta_c R_b W n_{ps}}. \tag{18}$$

Total area of collection,

$$A_{c\ tot} = n_{ps}BL. \tag{19}$$

The irreversibility of each component/processes can be determined either from exergy balance or Guoy–Stodola equation. The following are the irreversibility equations for cycle components.

Irreversibility of mixture turbine,

$$I_{MXT} = m_1\ T_0\ (s_2 - s_1). \tag{20}$$

Irreversibility of condensate pump,

$$I_{CDP} = m_9 T_0 \, (s_{10} - s_9) \, . \tag{21}$$

Irreversibility of subcooler,

$$I_{subcooler} = m_3 \, (e_3 - e_4) + m_6 \, (e_6 - e_7) \, . \tag{22}$$

where, the specific exergy, $e = h - T_0 \, s$.

Irreversibility of solution heat exchanger,

$$I_{solutionHEX} = m_{10} \, (e_{10} - e_{11}) + m_{13} \, (e_{13} - e_{14}) \, . \tag{23}$$

Irreversibility of throttling devices,

$$I_{THRI} = m_4 \, (e_4 - e_5) \tag{24}$$

$$I_{THRII} = m_{14} \, (e_{14} - e_{15}) \tag{25}$$

Irreversibility of heat recovery vapour generator (HRVG),

$$I_{HRVG} = m_{11} \, (e_{11} - e_{12}) + m_{16} \, (e_{16} - e_1) + m_{23} \, (e_{23} - e_{25}) \, . \tag{26}$$

Irreversibility of separator,

$$I_{SEP} = m_{12} e_{12} - m_{13} e_{13} - m_{16} e_{16}. \tag{27}$$

Irreversibility of condenser,

$$I_{CND} = m_2 \, (e_2 - e_3) + m_{17} \, (e_{17} - e_{18t}) \, . \tag{28}$$

Irreversibility of absorber,

$$I_{ABS} = m_8 \, (e_8 - e_9) + m_{19} \, (e_{19} - e_{20}) \, . \tag{29}$$

Irreversibility of evaporator,

$$I_{EVP} = m_5 \, (e_5 - e_6) + m_{21} \, (e_{21} - e_{22}) \, . \tag{30}$$

Total irreversibilities in combined cycle,

$$\begin{aligned} I_{tot} \; = \; & I_{MXT} + I_{CDP} + I_{subcooler} + I_{solution\ HEX} + I_{THR\ I} + I_{THR\ II} + I_{HRVG} \\ & + I_{SEP} + I_{CND} + I_{ABS} + I_{EVP}. \end{aligned} \tag{31}$$

The supply exergy to the cycle is the exergy value of the hot fluid at the collector exit temperature.

$$E_{hf} = (h_{23} - h_0)_{hf} - T_0 \, (s_{23} - s_0)_{hf} \, , \tag{32}$$

where h_0 and s_0 are specific enthalpy and specific entropy of hot fluid at the reference point.

Power output from the mixture turbine,

$$w_t = m_1 \, (h_1 - h_2) \, \eta_t \, \eta_{gen.} \tag{33}$$

Power to pump,

$$w_p = \frac{m_9(h_{10} - h_9)}{\eta_p}. \tag{34}$$

Net power output,

$$w_{net} = w_t - w_p. \tag{35}$$

Refrigerating effect,

$$q_{EVP} = m_5 (h_6 - h_5). \tag{36}$$

For plant energy values, the actual mass can be multiplied to convert from specific values to total values.
Integrated cycle EUF,

$$EUF_{cycle} = \frac{w_{net} + q_{EVP}}{q_g + q_{SH}}. \tag{37}$$

Solar plant EUF,

$$EUF_{plant} = \frac{W_{net} + Q_{EVP}}{R_g A_{tot\ c}}. \tag{38}$$

Integrated cycle power efficiency,

$$\eta_{cycle} = \left(\frac{w_{net}}{q_g + q_{SH}}\right) \times 100 \tag{39}$$

Power plant energy efficiency,

$$\eta_i = \left(\frac{W_{net}}{R_g A_{tot\ c}}\right) \times 100. \tag{40}$$

3. Results and discussions

The operational conditions for the proposed plant are different when compared to power only or cooling only plant. Many trials have been carried out to find the lower and upper limits of feasible operational conditions. The processes conditions (HP and vapour fraction) have been studied to justify and analyse the changes in plant performance.

Figure 3 shows the influence of strong solution with separator temperature on plant's HP and vapour fraction. Since the vapour fraction depends on concentrations (strong solution concentration and weak solution concentration), an increase in separator temperature only increases the HP but not the vapour fraction. HP has been evaluated at the saturated liquid solution at the separator exit. Therefore, it is a function of separator concentration and strong solution concentration. It also changes (decreases at high temperatures) with concentration as shown in figure. The IP and LP remain unchanged due to the fixation of exit conditions at condenser and evaporator. The HP has been increased from 0.1 bar to 3.75 bar at IP and LP values of 0.07 bar and 0.01 bar, respectively.

Figure 4 shows the influence of strong concentration (0.58–0.62) with separator temperature (90–200°C) on cycle energy utilization factor (EUF), plant EUF, specific power and specific cooling, cycle power efficiency, cycle coefficient of performance (COP), total output and specific area of solar collectors. The strong solution should not exceed above 0.66 due to crystallization

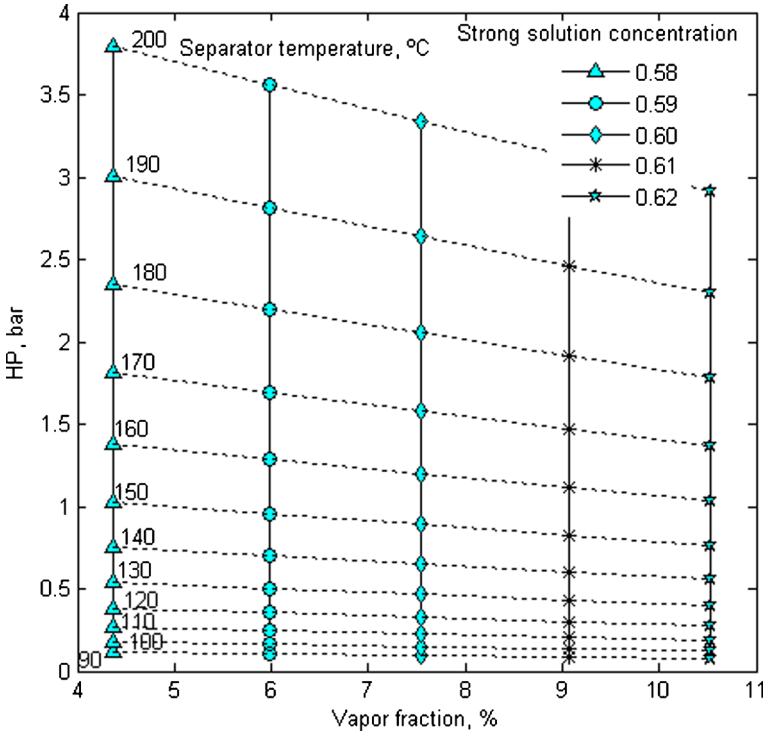

Figure 3. Changes in plant HP and vapour fraction with strong solution concentration and separator temperature.

line. The maximum concentration for strong solution is maintained much below the crystallization point to overcome the crystallization problem. Higher generator temperature and extreme concentration of the solutions lead to crystallization. The temperature limits for separator has been fixed as per the feasibility of operational conditions. It is evident that high strong solution concentration favours both power and cooling. But increase in separator temperature supports power and its efficiency but not cooling and its efficiency (COP). The plant EUF increases and maximizes with a minimum specific solar collector's area up to 140–150°C of separator temperature. The influence of strong solution is diminishing with its increase on efficiencies and outputs. Xu *et al* (2000) reported a 100 kW of total output (75 kW power and 25 kW cooling) at the cycle source and sink temperatures of 140°C and 7°C, respectively with aqua ammonia as a working fluid. The new plant results 150 kW of total output (20 kW power and 130 kW of cooling) at the cycle source and sink temperatures of 140°C and 40°C, respectively with 59% strong solution concentration with LiBr–water mixture. Due to change in sink temperature from 7 to 40°C, the amount of power generated is low when compared to the Goswami cycle. But more cooling has been produced by new plant because LiBr–water mixture gives high COP (0.75) compared to aqua ammonia mixture (0.3). The cycle EUF and plant EUF varies from 0.7 to 0.87 and 0.3–0.345, respectively with the above stated changes. The specific power and specific cooling (refrigeration effect) increases respectively from 1 to 50 kW and 100–260 kW. The cycle power efficiency and cooling efficiency variations are 1–14% and 0.64–0.77, respectively. Since the total output increases from 100 to 300 kW with increase in concentration, the collector area minimizes from 3.4 to 3 m^2 kW^{-1} of total output. On overall basis, the maximum feasible strong

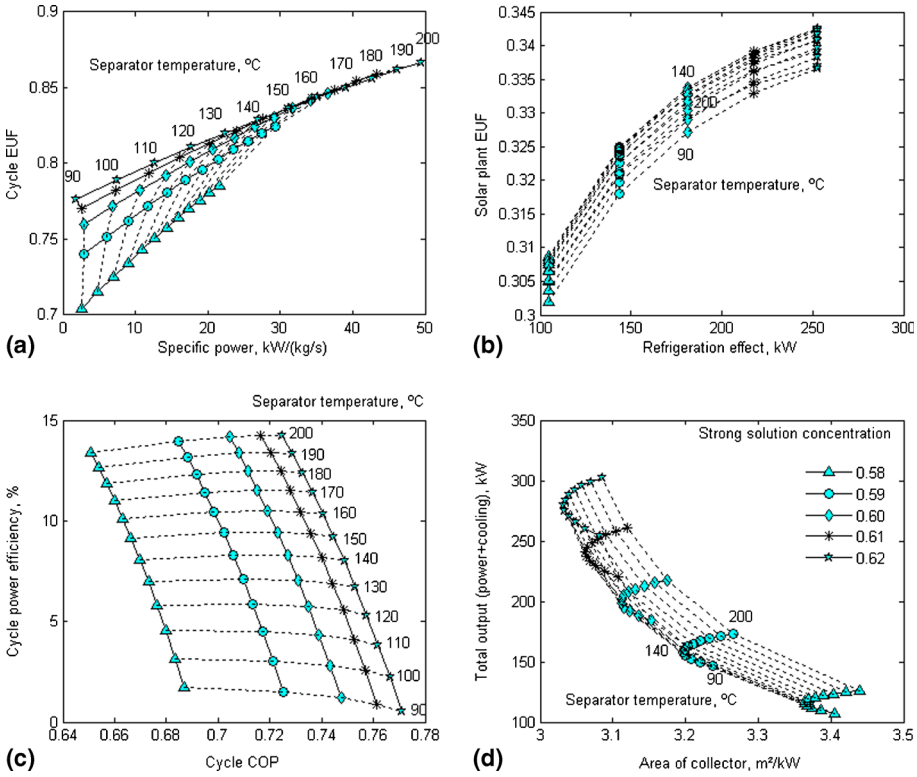

Figure 4. Influence of strong solution concentration and separator temperature on (**a**) cycle EUF-specific power, (**b**) plant EUF-refrigeration effect, (**c**) cycle power efficiency-cycle COP and (**d**) total output-specific area of collectors.

solution concentration with a separator temperature of 150°C has been recommended to get higher total output with a minimum solar collector's area.

Figure 5 shows the effect of strong solution concentration (0.6–0.62) and cooling water inlet temperature (24–30°C) on plant conditions. HP is fixed at constant circulating cooling water temperature and is a function of strong solution concentration and separator temperature. The lower cooling water inlet temperature results high vapour fraction in separator so more quantity of steam for power and cooling. It results in high EUF at low sink temperature. The HP decreased from 0.89 to 0.76 bar with an increase in strong solution concentration. The vapour fraction changed from 7 to 16.5% with strong solution concentration and sink temperature variations.

Figure 6 gives the influence of strong solution concentration and circulating cooling water inlet temperature. The cooling water inlet temperature has been varied from 24 to 30°C with 8 K as a TTD in condenser and absorber which limits from strong solution concentration. It demands high strong solution concentration above 30°C of cooling water inlet temperature which is not feasible due to crystallization limit. The performance (cycle EUF, plant EUF, specific power, specific cooling, cycle power efficiency, cycle COP and total output) decreases with an increase in sink temperature (circulating water inlet temperature) as per the thermodynamics. Therefore, the collector's area increases with rise in sink temperature. The plot also proves the advantage of high concentration for strong solution to result more output. The sink temperature influence is high at high temperature on plant performance. With the increase in cooling

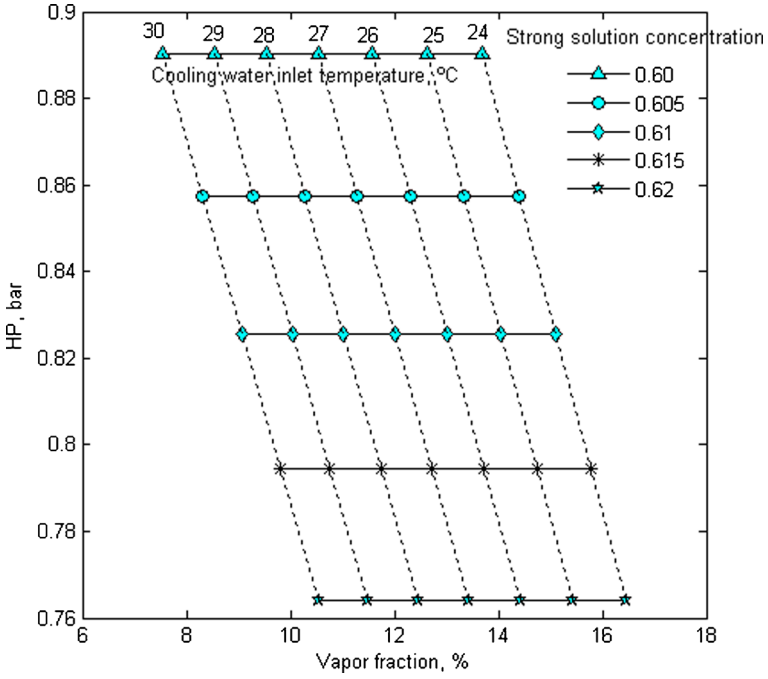

Figure 5. Changes in plant HP and vapour fraction with strong solution concentration and circulating cooling water inlet temperature.

water inlet temperature, the changes in cycle EUF, plant EUF, specific power, specific cooling, cycle power efficiency, cycle cooling efficiency (COP), total output and specific area respectively are 0.89–0.82, 0.36–0.34, 50–25 kW, 400–200 kW, 11.5– 9.5%, 0.78–0.72, 450–200 kW and 2.85–3.1 $m^2\ kW^{-1}$.

Figure 7 compares the exergetic losses occurred in each component/processes of the proposed cycle. It helps in the assessment of strong and weak areas of the proposed plant. It also checks the correctness of the thermodynamic evaluation by exergy balance. The net entropy will always increase in thermodynamic processes of a component. If it is not so, the exergetic loss becomes negative and indicates an error in the evaluation of component. The positive values of all the components shown in figure ensure the correctness of the evaluation. The major exergetic (15.5%) losses occur in HRVG due to consideration of high TTD compared to other heat exchangers. The other exergetic losses are below 2% of exergy of hot fluid. The results also prove the advantage of mixtures compared to pure substance (as pure substance gives more exergetic loss). At evaporator, absorber and condenser the percentage in exergetic losses are approximately 1% each. The total exergetic losses are approximately 21% of exergy of hot supply fluid i.e., it results 79% of exergy efficiency.

Table 2 gives the results of the specifications of solar thermal integrated plant at the operating conditions stated at earlier sections. The rating of heat exchangers, power, efficiency and EUF are developed at the unit mass of the working fluid. These specifications are developed at the same conditions defined in table 1. The heat load in subcooler is low when compared to solution heat exchanger and the heat loss at absorber is more than the condenser. The cooling output is seven times more than the power output. The overall EUF for cycle and plant are 82% and 33%,

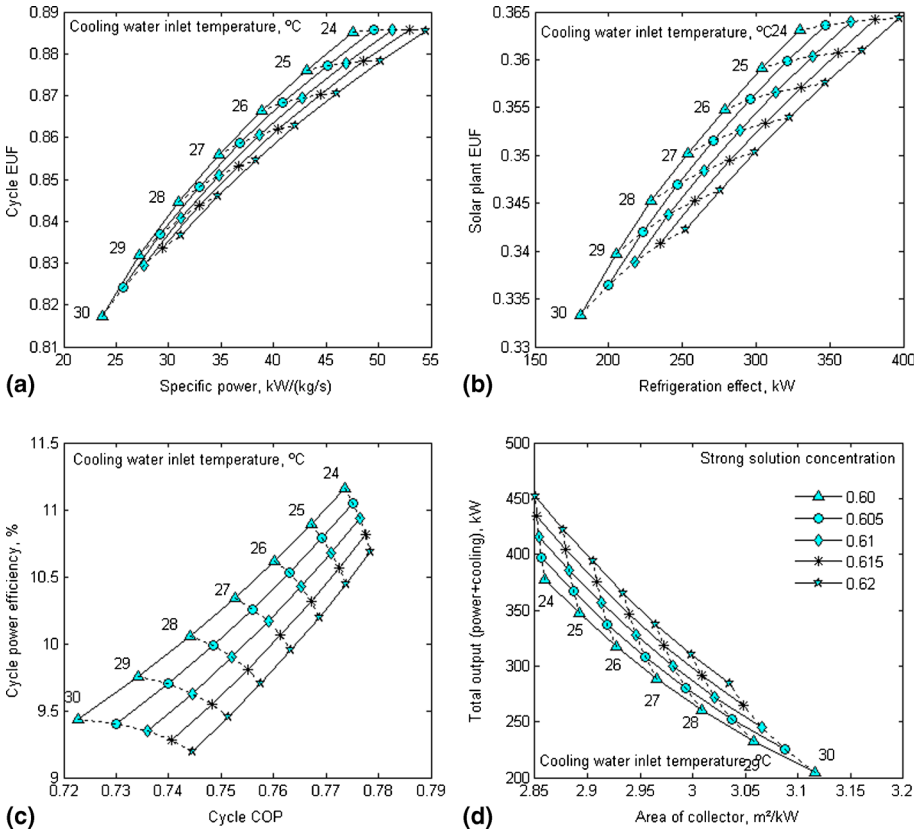

Figure 6. Influence of strong solution concentration and cooling water inlet temperature on (**a**) cycle EUF-specific power, (**b**) plant EUF-refrigeration effect, (**c**) cycle power efficiency-cycle COP and (**d**) total output-specific area of collectors.

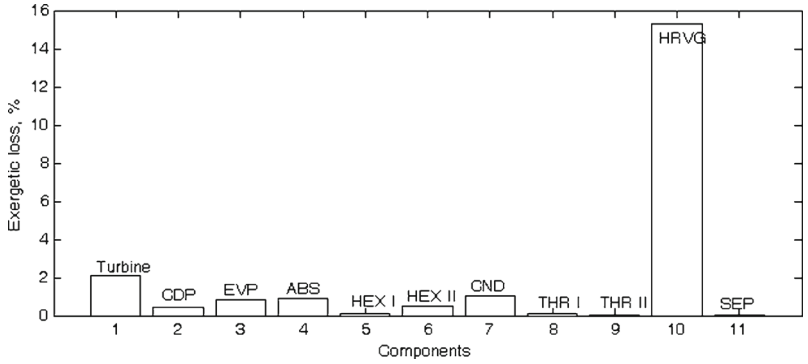

Figure 7. Comparison of exergetic losses in compound cycle components/processes; ABS: absorber, CDP: condensate pump, CND: condenser, EVP: evaporator, HRVG: heat recovery vapour generator, SEP: separator and THR: throttling.

Table 2. Specifications of the solar thermal power and cooling plant integrated with LiBr–H_2O working fluid at the separator temperature of 150°C, 0.6 strong solution concentration and unit mass of strong solution.

Description	Result
Solar radiation, W m^{-2}	700 (beam), 950 (global)
Generator heat load, kW	250
Superheater heat load, kW	2
Condenser heat load, kW	173
Subcooler heat load, kW	4
Solution heat exchanger heat load, kW	173
Evaporator heat load, kW	180
Absorber heat load, kW	233
Gross power from turbine, kW	25
Work input to solution pump, kW	0.5
Net specific power, kW	24.5
Refrigerating effect, TR	51 (180 kW)
COP	0.72
Collector efficiency, %	55.7
Power cycle energy efficiency, %	9.8
Solar plant power efficiency, %	4
Cycle energy utilization factor	0.82
Solar plant energy utilization factor	0.33
Cycle exergy efficiency, %	79
Total area of collectors, m^2 kW^{-1}	3

respectively. Based on total exergy losses in components/process, the second law efficiency has been found to be 79%.

Since the same category of integrated cycle is not available in the literature, the thermodynamic work has been validated by comparing the LiBr–water cooling results instead of the

Table 3. Validation of the simulation method by comparing current simulated values with literature results at separator liquid concentration of 0.6 and weak solution of 0.00517 kgs^{-1} (Florides *et al* 2003).

Description	Florides *et al* (2003)	Simulation	Error, %
High pressure, kPa	4.82	4.73	1.87
Low pressure, kPa	0.93	0.93	0
Separator inlet concentration	0.55	0.549	0.18
Separated vapour portion, kg s^{-1}	0.000431	0.0004	7.19
Separated liquid portion, kg s^{-1}	0.00474	0.0047	0.84
Temperature at exit of solution throttle vale , °C	44.5	53	−19.1
Temperature at exit of water throttle vale, °C	6	6	0
Solution exit temperature at subcooler	51.5	53.9	−4.66
Absorber exit temperature, °C	34.9	37.2	−6.6
Condenser exit temperature, °C	31.5	31.85	−1.11
Boiler heat input, kW	1.35	1.3577	−0.57
Absorber heat rejection, kW	1.28	1.32	−3.12
Condenser heat rejection, kW	1.07	1.0764	−0.6
Refrigeration capacity, kW	1	1.03	−0.03
Cycle COP	0.74	0.76	−2.7

integrated plant. Table 3 compares the simulated results of VAR with literature results at the same conditions to validate the proposed model work at same working fluid (Florides *et al* 2003). The same configuration and conditions have been considered for comparison of the reported results. The calculated results of pressures, temperatures, concentrations, heat duties and energy values have been compared and found satisfactory match between these two. The temperature at the exit of throttle valve has −19.1% of error. It is because of the relatively high throttle inlet temperature in the simulation. On overall basis, there is a good match between the calculated values and the literature results. This validation shows the correctness of the evaluation methodology and the results of the proposed model.

4. Conclusion

The proposed integrated plant has been evaluated and analysed with the focus on strong solution concentration, separator temperature and circulating cooling water inlet temperature to develop optimized working conditions. High strong solution concentration, medium separator temperature (140–150°C) and low sink temperature are recommended to result high EUF for both cycle and plant. The exergetic losses in components/processes in per cent of exergy of hot fluid have been compared and the major exergetic loss (15%) has been observed at the HRVG. The resulted cycle EUF, plant EUF, specific power, specific cooling, cycle power efficiency, cycle COP and solar collector area at 150°C of separator temperature are 82%, 33%, 25 kW, 180 kW, 10%, 0.72 and 3 m^2kW^{-1} total output, respectively. Nearly 80% cycle exergy efficiency can be expected from the new integrated plant.

Nomenclature

A	Area, m^2
a	Ambient
B	Width of collector, m
e	Specific exergy, kJ kg^{-1}
E	Exergy, kJ
EUF	Energy utilization factor
h	Specific enthalpy, kJ kg^{-1}
I	Irreversibility, kJ
L	Length, m
m	Mass, kg s^{-1}
N	Number
q	Specific heat, kJ kg^{-1}
Q	Heat, kJ
R	Solar radiation, W m^{-2}
s	Specific entropy, kJ kg^{-1} K^{-1}
T	Temperature, K
TTD	Terminal temperature difference, K
W	Work output, kJ
VF	Vapour fraction
x	Mass fraction of LiBr in mixture, kg kg^{-1}
η	Efficiency
λ	Circulation ratio

Subscripts

0	Reference state (25°C and 1 atm.)
ABS	Absorber
b	Beam
c	Collector
CND	Condenser
EVP	Evaporator
g	Global
gen	Generator
hf	Hot fluid
HEX	Heat exchanger
HRVG	Heat recovery vapour generator
m	Mechanical
MXR	Mixture
MXT	Mixture turbine
p	Pump
ps	Parallel segments
ref	Refrigerant
SEP	Separator
SH	Superheat
ss	Strong solution
t	Turbine
THR	Throttling
tot	Total
ws	Weak solution

References

Aphornratana S and Sriveerakul T 2007 Experimental studies of a single-effect absorption refrigerator using aqueous lithium–bromide: Effect of operating condition to system performance. *Expt. Therm. Fluid Sci.* 32(2): 658–669

Florides G A, Kalogirou S A, Tassou S A and Wrobel L C 2003 Design and construction of a LiBr–water absorption machine. *Energy Conv. Mangt.* 44(15): 2483–2508

Ishida T, Kawano S, Kohtaka I, Yamada K, Kaku H and Narita T 1991 Hybrid Rankine cycle system. *USP* 5007240: 1–12

Jawahar C P, Saravanan R, Bruno J C and Coronas A 2013 Simulation studies on gax based Kalina cycle for both power and cooling applications. *Appl. Therm. Eng.* 50(2): 1522–1529

Kaita Y 2001 Thermodynamic properties of lithium bromide-water solutions at high temperatures. *Int. J. Refrig.* 24(5): 374–390

Misra R D, Sahoo P K, Sahoo S and Gupta A 2003 Thermoeconomic optimization of a single effect water/LiBr vapour absorption refrigeration system. *Int. J. Refrig.* 26(2): 158–169

Sreeramulu M, Gupta A V S S K S and Srinivas T 2011 Exergy analysis of gas turbine – solid oxide fuel cell-based combined cycle power plant. *Int. J. Energy Technol. Policy* 7(5/6): 469–488

Srinivas T and Vignesh D 2012 Performance enhancement of GT-ST power plant with inlet air cooling using lithium bromide/water vapour absorption refrigeration system. *Int. J. Energy Technol. Policy* 8(1): 94–107

Srinivas T, Reddy B V and Gupta A V S S K S 2011 Biomass fueled integrated power and refrigeration system. *Proc. Inst. Mech. Eng. Part A: J. Power Energy* 225(3): 249–258

Srinivas T, Reddy B V and Gupta A V S S K S 2012 Thermal performance prediction of a biomass based integrated gasification combined cycle plant. *ASME J. Energy Resources Technol.* 134(2): 1–9

Sun D W 1997 Thermodynamic design data and optimum design maps for absorption refrigeration systems. *Appl. Therm. Eng.* 17(3): 211–221

Talbia M M and Agnew B 2000 Exergy analysis: An absorption refrigerator using lithium bromide and water as the working fluids. *Appl. Therm. Eng.* 20(7): 619–630

Tamm G and Goswami D Y 2003 Novel combined power and cooling thermodynamic cycle for low temperature heat sources, Part 2: Experimental investigation. *ASME J. Sol. Energy Eng.* 125(2): 223–229

Tamm G, Goswami D Y, Lu S and Hasan A A 2003 Novel combined power and cooling thermodynamic cycle for low temperature heat sources, Part 1: Theoretical investigation. *ASME J. Sol. Energy Eng.* 125(2): 218–222

Tamm G, Goswami D Y, Lu S and Hasan A A 2004 Theoretical and experimental investigation of an ammonia–water power and refrigeration thermodynamic cycle. *Solar Energy* 76(1–3): 217–228

Valan Arasu A and Sornakumar T 2007 Design, manufacture and testing of fiberglass reinforced parabola trough for parabolic trough solar collectors. *Solar Energy* 81(10): 1273–1279

Vidala A, Bestb R, Riveroc R and Cervantes J 2006 Analysis of a combined power and refrigeration cycle by the exergy method. *Energy* 31(15): 3401–3414

Wang J, Dai Y and Gao L 2008 Parametric analysis and optimization for a combined power and refrigeration cycle. *Appl. Energy* 85(11): 1071–1085

Wang J, Dai Y, Zhang T and Ma S 2009 Parametric analysis for a new combined power and ejector–absorption refrigeration cycle. *Energy* 34(10): 1587–1593

Xu F, Goswami Y D and Bhagwat S S A 2000 Combined power/cooling cycle. *Energy* 25(3): 233–246

Zhang C, Yang M, Lu M, Shan Y and Zhu J 2011 Experimental research on LiBr refrigeration - Heat pump system applied in CCHP system. *Appl. Therm. Eng.* 31(17–18): 3706–3712

Zheng D, Chen B, Qi Y and Jin H 2006 Thermodynamic analysis of a novel absorption power/cooling combined cycle. *Appl. Energy* 83(4): 311–323